JOURNAL OF SOLID STATE CHEMISTRY 32, 311–319 (1980)

The Structure of the Low-Temperature γ-Modification of $Cs_2PbCu(NO_2)_6$: A Powder Neutron Diffraction Study at 160 K

S. KLEIN AND D. REINEN

Sonderforschungsbereich 127 and Fachbereich Chemie der Universität, Marburg, Lahnberge, West Germany

Received January 24, 1979; in revised form July 23, 1979

A powder neutron diffraction study on the low-temperature modification of $Cs_2PbCu(NO_2)_6$ yielded a monoclinic unit cell [space group $B2/b$ with $a' = 773.4(3)$ pm, $b' = 1553.1(6)$ pm, $c' = 2137.6(8)$ pm, $\gamma' = 90.10(1)$, and $Z = 8$], which deviates only slightly from tetragonal. Though a thorough structure determination was not possible, the essential features of the structure are clearly revealed. The CuN_6 octahedra are tetragonally elongated with a small orthorhombic component superimposed [bond lengths $\perp c'$, 211.5 pm ($2x$) and 230 pm ($2x$); $\parallel c$, 207 pm]. The cooperative Jahn–Teller order pattern corresponds to the antiferrodistortive model.

1. Introduction

Lead nitrocomplexes $A^{\mathrm{I}}_2PbCu(NO_2)_6$ (A^{I}: K, Rb, Tl, Cs) exhibit successive first-order phase transitions, which are induced by static and dynamic Jahn–Teller effects (*1–3*). For $Cs_2PbCu(NO_2)_6$ the following modifications and transition temperatures were found by EPR spectroscopy (*2*) and confirmed by single-crystal neutron diffraction analyses (*4–6*), thermochemical analysis (*7*), ir spectroscopy, and polarization microscopy (*5*):

$$\underset{\text{mon}}{\gamma} \underset{275\,\text{K}}{\overset{289\,\text{K}}{\rightleftharpoons}} \underset{\text{o-rh}}{\beta'}{}^{1} \underset{294\,\text{K}}{\overset{310\,\text{K}}{\rightleftharpoons}} \underset{\text{o-rh}}{\beta} \underset{389\,\text{K}}{\overset{398\,\text{K}}{\rightleftharpoons}} \underset{\text{cub}}{\alpha}.$$

While the cubic α-phase contains dynamically distorted CuN_6 polyhedra (*6*), a partially planar dynamic Jahn–Teller effect, based on elongated CuN_6 octahedra, is suggested for the β- and β′-modifications (*2-4*).[2] For the low-temperature γ-modification finally an antiferrodistortive order of tetragonally elongated CuN_6 octahedra (possibly with a small orthorhombic component) was proposed from powder and single-crystal EPR data (*1, 2, 9*). A rigorous single-crystal structure determination proved to be very difficult, because the complications, which arise from twinning and the development of domain structures below the relevant phase transitions are even greater for the γ- than for the β(β′)-modifications. Thus we decided to perform a neutron diffraction powder investigation with the aim of revealing the essential structural features of the γ-phase.

2. Experimental

Neutron diffraction diagrams were taken at 160 K (Fig. 1) and 300 K with the high-resolution diffractometer D1A installed at the ILL in Grenoble, using a wavelength of 298 m. A helium cryostat provided with a

[1] Compare Table III and discussion, however.

[2] A different description is proposed in (*8*) (compare discussion).

0022-4596/80/060311-09$02.00/0

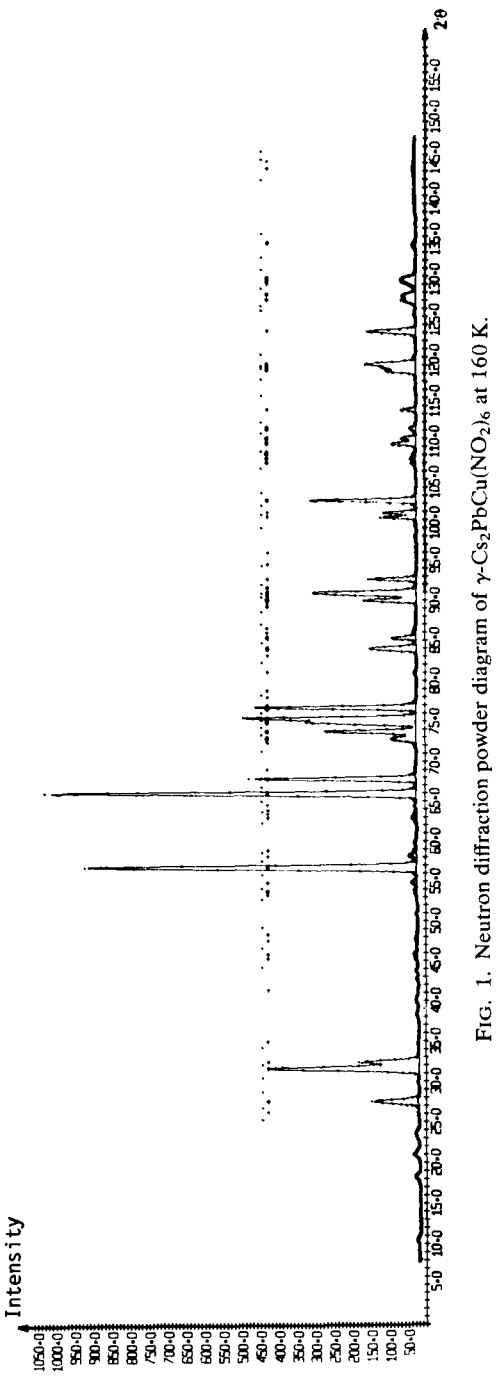

FIG. 1. Neutron diffraction powder diagram of γ-$Cs_2PbCu(NO_2)_6$ at 160 K.

heating system in the sample space was used for temperature control. The measurements were made in the range of Bragg angles $7.6° \leq 2\Theta \leq 147.0°$ with steps of $\Delta 2\Theta = 0.05°$. The monochromator used was a germanium single crystal with the (111) plane in the reflective position. In addition to the normal reflections relatively strong $\lambda/3$ reflections appear, from which the most intensive are those at $2\Theta = 18.1$, 20.8, and 23.3°. Due to the great wavelength of 298 pm and the high resolution of the diffractometer, we were able to detect a monoclinic angle deviating but little from 90°. While reflections *hkl* [orthorhombic indexing] with large values of *h* and *k* are considerably broadened as compared with reflections having small values of *h* and *k* (Fig. 2: reflections 331, 242, 333 in comparison to 131, 204, 115, 404), the 440 reflection is distinctly split into the two components $\bar{4}40$ and 440. From this splitting a monoclinic angle of $\gamma = 90.2 \pm 0.05°$ is calculated. But even when a monoclinic unit cell is chosen [$a = 1096.8(4)$ pm; $b = 1095.4(4)$ pm; $c = 1068.8(4)$ pm; $\gamma = 90.20(5)°$; $Z = 4$] and the $\lambda/3$ reflections are taken into account, there are still additional reflections in the powder diagram, from which in particular those at $2\theta = 58.1$ and 62.8° differ significantly from the back-

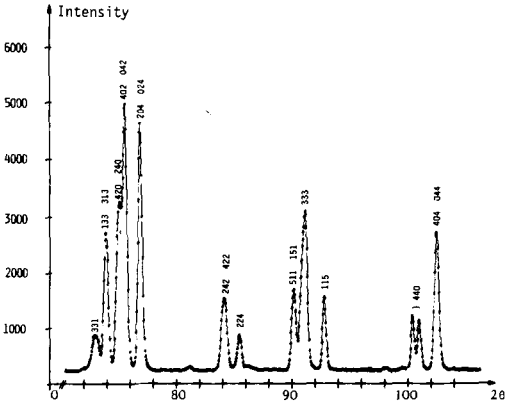

FIG. 2. Part of the diagram in Fig. 1 (orthorhombic indices).

ground (Fig. 3). They do not originate from *Al*, however, but can be indexed as $\frac{7}{2}\frac{1}{2}\frac{1}{2}$ and $\frac{7}{2}\frac{3}{2}\frac{1}{2}$; hence the *a*-, *b*-, and *c*-axes of the monoclinic unit cell have to be doubled.

The powder sample of $Cs_2PbCu(NO_2)_6$ was prepared by the usual procedure (*1*). It was recrystallized several times, however, to make sure that the observed superstructure reflections were not due to impurities.

3. Structural Refinement

Starting with a monoclinic cell $[2a, 2b, 2c, \gamma]$ which has eight times the volume of the orthorhombic pseudocell $[a, b, c]$, we have 112 free local parameters and 88 free isotropic temperature parameters at our disposal in the model with the highest symmetry. These 200 free parameters are matched by only 47 separable groups of reflections; therefore, a reasonable refinement can be made but stepwise.

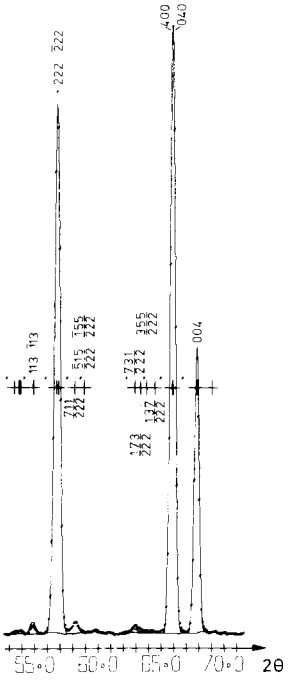

FIG. 3. Part of the diagram in Fig. 1 (orthorhombic indices).

(*a*) *Refinement in the Orthorhombic Space Group Fmmm*

In the first step the splitting of the 440 reflection and the broadening of the reflections with high values of *h* and *k* are not taken into account, as well as the existence of $\lambda/3$ and superstructure reflections. In the so-defined pseudocell $[a, b, c]$ of space group *Fmmm* ($Z = 4$) the following atomic positions are occupied:

$$\begin{aligned} &\text{Cu: } 4a; \quad \text{Pb: } 4b; \quad \text{Cs: } 8f, \\ &\text{N: } 8g, 8h, 8i; \quad 0: 16m, 16n, 16o. \end{aligned} \tag{1}$$

The number of free parameters is reduced to nine positional and nine isotropic temperature parameters. The refinement yields the following integral quality factors:

$$R_F = \frac{\sum_{hkl} \| |F_{hkl}^{obs}| - |sF_{hkl}^{calc}| \|}{\sum_{hkl} |F_{hkl}^{obs}|} = 0.025,$$

without $|F_{hkl}^{obs}| < 2\sigma$,

$$R_I = \frac{\sum_{hkl} |I_{hkl}^{obs} - sI_{hkl}^{calc}|}{\sum_{hkl} I_{hkl}^{obs}} = 0.041.$$

The profile reliability factor

$$R_P = \frac{\sum_{2\Theta} |I_{2\Theta}^{obs} - sI_{2\Theta}^{calc}|}{\sum_{2\Theta} I_{2\theta}^{obs}}$$

breaks down into

$R_P^{obs} = 0.220$ and $R_P^{calc} = 0.223$, respectively (*10*).

The reliability factors R_F and R_I are so extremely low that the violation of all-face centering in the monoclinic γ-phase can be but minor. The major difference with respect to the (partially dynamic) $\beta(\beta')$-phase (*4*) lies in the Cu–N bond lengths in the (001) plane. *These distances are identical within the*

error limits in the β-modification [223.0((3) pm], but different in the γ-phase, with the spacing Cu–N_3 [225.8(9) pm] in the direction of the b-axis greatly exceeding the spacing Cu–N_2 [215.0(2) pm] in the direction of the a-axis. This would imply, at the first glance, that the Cu–N bond lengths along the *a*-axis are always short, while they are always long in the *b*-direction—a result which is not in agreement with the nearly identical lattice parameters $a = 1096.8(4)$ pm and $b = 1095.4(4)$ pm. The inconsistency can be met by the assumption, however, that the same number of short and long Cu–N spacings occurs in the direction of the *a*- and *b*-axis, respectively.

Though the refinement was based on the atomic parameters of the β-phase with two identical Cu–N spacings, two different bond lengths were obtained. If, as has been assumed, short *and* long Cu–N bond lengths appear in the *a*- (and *b*)-direction, two atomic *N* positions [N_2, N_3 along *a* and N_2', N_3' along *b*] with weight $\frac{1}{2}$ might give better agreement between calculated and observed intensities than average positions with the weight of 1. However, since reflections *hkl* superimpose with reflections *khl* in the powder diagram due to $a \approx b$, the calculations yielded identical results. Also, there was no difference in calculations based on Cu–N_3 < Cu–N_2 or, alternatively, Cu–N_2 < Cu–N_3. The proposed model will be discussed in more detail, when the superstructure reflections are included in the refinement.

(b) λ/3 Correction

From the intensity of the three λ/3 reflections at $2\theta = 18.1$, 20.8, and 23.3° a scaling factor can be determined for the λ/3 correction. The calculations were also performed in the *Fmmm* space group. The error caused by neglecting the small deviation of γ from 90° is very small, since the strongest λ/3 reflections lie at low Bragg angles 2Θ. By the λ/3 correction the profile reliability factors were improved to:

$$R_P^{obs} = 0.192 \quad \text{and} \quad R_P^{calc} = 0.190.$$

(c) Refinement Including the Monoclinic Angle

While the integral reliability factors R_F and R_I are expected to change only slightly, if the monoclinic angle $\gamma = 90.2°$ is taken into account, a considerable improvement is expected for the profile R_P factors. The monoclinic angle implies that the positions of the *hkl* and $\bar{h}kl$ reflections no longer coincide exactly. Hence, the $\bar{h}kl$ reflections were taken into account in the calculation in addition to the *hkl* reflections of *Fmmm*. Though this procedure does not correlate with a definite crystallographic space group, it should be allowed as an intermediate stage within the stepwise refinement. As a matter of fact, this calculation refines the monoclinic angle to $\gamma = 90.23(1)°$ and leads to considerably lower R_P factors:

$$R_P^{obs} = 0.112 \quad \text{and} \quad R_P^{calc} = 0.117.$$

(d) The Structural Model and Final Refinement

The inclusion of the superstructure reflections (Fig. 3) into the refinement improves the profile quality factors considerably (see below). The existence of such reflections leads to a doubling of the *a*-, *b*-, and *c*-axes and proves that the sequence of short and long Cu–N spacings along *a* and *b* is not statistical. A possible (idealized) model for an ordered structure of this kind is shown in Fig. 4. It is based on an *antiferrodistortive* ordering pattern of tetragonally elongated CuN_6 octahedra (possibly with a small orthorhombic component). Long and short Cu–N bond lengths alternate in mutually perpendicular directions in the (001) plane. Because the lattice constant along *c* is twice as large as in the small cell (*a*, *b*, *c*, γ), a rotation of layers with analogous site distributions, which succeed one another along [001] ($z = 0, \frac{1}{2}, 1$), by 90° with respect to each

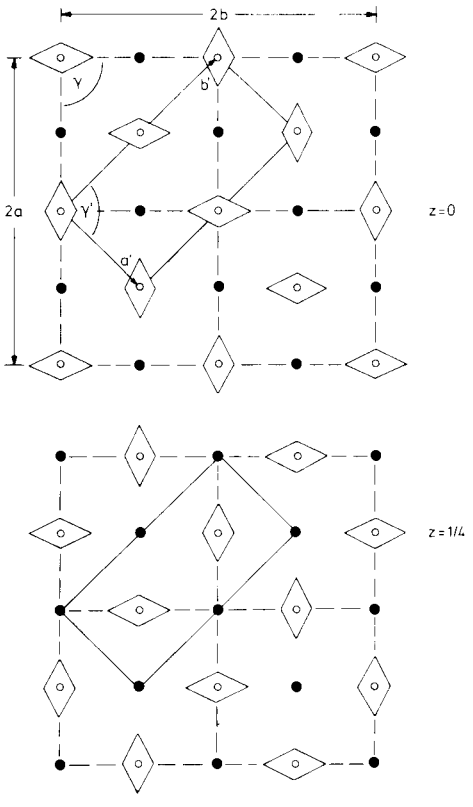

FIG. 4. Model of superstructure cell for γ-$Cs_2PbCu(NO_2)_6$ [$2a$, $2b$, $2c$, γ; $Z = 32$] with an antiferrodistortive order of elongated CuN_6 octahedra: (001) layers. (Layer in $z = \frac{1}{2}$ is rotated by 90° around [001] with respect to $z = 0$; smallest superstructure cell [a', b', c', γ'; $Z = 8$] is indicated.)

other has to be assumed. The lattice parameter $c = 1068.8(4)$ pm which is smaller than a and b by 27 pm does not allow short and long Cu–N bond lengths to alternate along the c-direction in the same way as along a and b in a reasonable model.

If these general structural principles are accepted, a superstructure of the space group $B2/b$ results. *Models with lower symmetries will not be treated, in order to keep the number of free parameters as low as possible.* In the space group $B2/b$ the smallest unit cell has the dimensions $a' = 773.4(3)$ pm; $b' = 1553.1(6)$ pm; $c' = 2c$; $\gamma' = 90.10(1)°$ with $Z = 8$ (Fig. 4) and results from the large cell by applying the transformation matrix:

$$\begin{pmatrix} \frac{1}{4} & \frac{1}{4} & 0 \\ -\frac{1}{2} & \frac{1}{2} & 0 \\ 0 & 0 & 1 \end{pmatrix}$$

The following description is still based on the pseudocell with $2a$, $2b$, $2c$, γ, however, because this allows an easy comparison with the unit cells of the α- and β-phases. It is composed of eight Cu^{2+} sublattices, from which always two are coupled corresponding to an antiferrodistortive ordering pattern. These four pairs, which can be chosen independently in the orientation with respect to one another, are [in $B2/b$ with equivalent positions $(0\ 0\ 0;\ \frac{1}{2}\ 0\ \frac{1}{2})+$]:

$0\ 0\ 0,\ 0\ \frac{1}{2}\ \frac{1}{2}$ and $0\ \frac{1}{2}\ 0,\ 0\ 0\ \frac{1}{2}$;

$\frac{1}{4}\ \frac{1}{2}\ \frac{1}{4},\ \frac{1}{4}\ 0\ \frac{3}{4}$ and $\frac{1}{4}\ 0\ \frac{1}{4},\ \frac{1}{4}\ \frac{1}{2}\ \frac{3}{4}$;

$0\ \frac{3}{4}\ \frac{1}{4}.\ 0\ \frac{1}{4}\ \frac{3}{4}$ and $0\ \frac{1}{4}\ \frac{1}{4},\ 0\ \frac{3}{4}\ \frac{3}{4}$;

$\frac{1}{4}\ \frac{1}{4}\ \frac{1}{2},\ \frac{1}{4}\ \frac{3}{4}\ 0$ and $\frac{1}{4}\ \frac{3}{4}\ \frac{1}{2},\ \frac{1}{4}\ \frac{1}{4}\ 0.$ (2)

They may arrange corresponding to eight possible models, from which one is shown in Fig. 4. Each of these superstructure cells has 112 free local parameters and 88 free isotropic temperature parameters. The number of the free parameters can be substantially reduced by taking into account strong correlations, however. The good agreement between calculated and observed integral intensities already in Section 3a proves, indeed, that the deviations from the equivalent positions in the orthorhombic *Fmmm* structure (a, b, c) are very small. For instance, we may assume the general position 0.001(1) 0.500(1) 0.500(1) for Cu^{2+} instead of the special coordinates $0\ \frac{1}{2}\ \frac{1}{2}$, which were

used in *Fmmm*. We can introduce the following general positions for one of the eight possible models then, which are strongly correlated with $x\,y\,z$:

$$\begin{array}{lll} x+0.000(1) & y+0.500(1) & z+0.500(1) \\ x+0.250(1) & y+0.000(1) & z+0.250(1) \\ x+0.250(1) & y+0.500(1) & z+0.750(1) \\ x+0.000(1) & y+0.250(1) & z+0.750(1) \\ x+0.000(1) & y+0.750(1) & z+0.250(1) \\ x+0.250(1) & y+0.250(1) & z+0.000(1) \\ x+0.250(1) & y+0.750(1) & z+0.500(1) \end{array} \quad (3)$$

The quality factors obtained are

$$R_I = 0.063, \quad R_F = 0.040,$$
$$R_P^{obs} = 0.081, \quad R_P^{calc} = 0.102.$$

The deterioration of the integral quality factors as compared with those of Sections 3a and 3c is caused by the extremely low intensities of the superstructural reflections with regard to the main reflections. If the superstructure reflections are considered alone a value R_I of about 0.50 is obtained.

The refined local parameters $x\,y\,z$ have been listed in Table I together with the isotropic temperature parameters. Further strong correlations beyond those listed in Eq. (3) exist between $x\,y\,z$ and $x+0.000(1)\ y+0.500(1)\ z+0.000(1)$ for Cs, Pb, Cu, N1, and O2 and are included in this table. The four free positional parameters of N2 as well as those of N3 could be reduced to two since, due to the identical lattice constants a and b within the limits of error, a short (long) Cu–N2 spacing along the a-axis should equal a short (long) Cu–N3 spacing along the b-axis. In the same way, the reduction in the number of free oxygen parameters can be justified. After all, only 9 free local parameters and 9 isotropic temperature parameters are left, which is actually a good relation with respect to the 47 reflection groups. The refinement within the unit cell with $Z = 8$ instead of the large cell (Fig. 4) does not further reduce the number of free parameters.

The coordinates in the monoclinic pseudocell [$2a, 2b, 2c, \gamma$; $Z = 32$] (Table I) can be transformed into those of the unit cell [a', b', c', γ'; $Z = 8$] by applying the matrix:

$$\begin{pmatrix} 2 & -1 & 0 \\ 2 & 1 & 0 \\ 0 & 0 & 1 \end{pmatrix}$$

4. Discussion and Summary

The way of refinement and the approximation with respect to "quasiequivalent" positions are justified by the good agreement reached between observed and calculated intensities. Bearing in mind the $\lambda/3$ correction and the very weak superstructural reflections, the profile quality factors can be regarded as satisfactory also. A distinction among the eight models from which one is shown in Fig. 4 was not possible, because the differences lie below the accuracy of measurement. The interatomic distances and bond angles of interest are listed in Table II and compared with the corresponding data of the α-, β-, and β'-phases. The mean values of the bond lengths for the different modifications are in very good agreement with each other [Cu–N, 217(1) pm; Pb–O, 284(1) pm; Cs–O, 321(2) pm; N–O, 125(2) pm; O–N–O: 116(2)°]. It is somewhat puzzling, however, that the static distortion of the CuN_6 polyhedra in the (001) planes of the structure (Fig. 4) is nearly entirely balanced by corresponding distortions of the NO_2 groups [two different N2–O2 and N3–O3 spacings as well as two O2–N2–O2 and O3–N3–O3 bond angles (Table II)] and affects the polarizable PbO_{12} polyhedra comparatively little. It seems to us that this result should not be taken as quantitatively significant, because it may be dominantly the

TABLE I

ATOMIC PARAMETERS AND (ISOTROPIC) TEMPERATURE FACTORS OF γ-$Cs_2PbCu(NO_2)_6$ [160 K][a]

	x	y	z	B
Cs	±0.125	±0.125	±0.125	1.3(9)
	±0.125	±0.625	±0.125	1.3
Pb	0	0	0.25	0.0(8)
	0	0.5	0.25	0.0
Cu	0	0	0	1.8(9)
	0	0.5	0	1.8
N1	0	0	±0.0969(6)	0.8(6)
	0	0.5	±0.0969	0.8
N2	±0.964(7)	0	0	0.7(5)
	±0.1050	0.5	0	0.9
N3	0	±0.1050(7)	0	0.9(6)
	0	±0.4036	0	0.7
O1	0	±0.0490(20)	±0.1251(14)	0.2(7)
	0	∓0.0490	±0.1251	0.2
	0	±0.5490	±0.1251	0.2
	0	±0.4510	±0.1251	0.2
O2	±0.1294(15)	0	∓0.0498(12)	0.2(9)
	±0.1294	0	±0.0498	0.2
	±0.1294	0.5	±0.0498	0.2
	±0.1294	0.5	∓0.0498	0.2
O3	±0.0467(12)	±0.1308(16)	0	1.2(8)
	∓0.0467	±0.1308	0	1.2
	±0.0467	±0.3692	0	1.2
	∓0.0467	±0.3692	0	1.2

[a] They refer to the large cell [$2a \approx 2b$, $2c$, γ; $Z = 32$] in space group $B2/b$. $(0\,0\,0; \frac{1}{2}\,0\,\frac{1}{2})+$ and the correlations given in Eq. (3) lead to equivalent positions.

consequence of the introduced correlations. The most interesting structural detail is certainly the considerable static deformation of the CuN_6 octahedra and the antiferrodistortive order pattern of these polyhedra. The distortion of the CuN_6 octahedra is somewhat smaller than the tetragonal elongation [204 pm ($4x$); 231 pm ($2x$)] in compounds $K_2M^{II}Cu(NO_2)_6$ (M^{II}: Ca^{2+}, Sr^{2+}, Ba^{2+}) (*11*) and has an orthorhombic component in addition.

The structural information available for the four modifications of $Cs_2PbCu(NO_2)_6$ is collected in Table III. While the high-temperature α-modification is three-dimensionally dynamic, the low-temperature γ-phase is the static version with an antiferrodistortive order of elongated CuN_6 octahedra (orthorhombic component superimposed). We proposed this cooperative Jahn–Teller order pattern for compounds $A^I_2PbCu(NO_2)_6$ in 1972 on the basis of EPR powder data (*1*)[3] and somewhat

[3] Figure 3 in (*1*) has to be corrected by introducing additional Cu^{2+} into the face-centered positions, however (*12*).

TABLE II

INTERATOMIC DISTANCES (pm) AND BOND ANGLES FOR THE MODIFICATIONS OF $Cs_2PbCu(NO_2)_6$

	γ^a	β, β'^b	α^c
Cu–N1	207.3(6)	207.3(6)	
–N2	211.5(7)	222.7(8)	217.4(7)
–N3	230.0(7)		
av	216.2	217.6	217.4
Pb–O1	288(2)	286(1)	
–O2	285(2)	285(1)	283(1)
–O3	281(2)	285(1)	
av	285	285	283
Cs–O1	320(2)	324.4(3)	
–O2	318(2)	321	322(1)
–O3	318(2)	318.6(4)	
av	319	321	322
N–O1	123(2)	124(1)	
–O2	129(2)	124(1)	
	119(2)		126.7(8)
–O3	117(2)	123(1)	
	127(2)		
av	123	124	127
O1–N1–O1	121(2)°	117(1)°	
O2–N2–O2	112(1)°		
	127(1)°	118(1)°	114(1)°
O3–N3–O3	107(2)°	116(1)°	
	122(2)°		
av	118°	117°	114°

[a] 160 K, this study.
[b] 293 and 323 K, respectively (*4, 5*).
[c] 420 K(*6*).

later EPR single-crystal data (*2, 9*). Though the structure of γ-$Cs_2PbCu(NO_2)_6$ could not be solved exactly, it should be correct in the *essential* details. In particular the coordinates of the metal cations (Pb^{2+}) may slightly deviate from the special positions of Table I, which were adopted in the process of refinement. The β- and β'-phases are intermediate stages. We concluded, from the angular dependence of the g-tensor, that the CuN_6 octahedra exhibit a (partially) planar dynamic Jahn–Teller effect [in (001) layers] in these modifications, leading to a tetragonally compressed coordination only in time average (*2, 3, 9*). The results of single-crystal studies by neutron diffraction are not in contradiction to this model (*4, 5*).

Mori *et al.* investigated particularly the satellite reflections, which appear in the β-, β'-, and γ-phases (*8*). They interpreted the results for the γ-modification by an antiferrodistortive order pattern analogous to the model we have found, but without giving any quantitative structural data. It is further stated in this paper that the β- and β'-modifications differ from the γ-phase by a partial (β', incommensurate phase) and complete disorder (β) along the [001] direction, respectively, while the (001) planes are still considered to be ordered in the antiferrodistortive pattern (Fig. 4). The last statement is not in agreement with the information of (partial) planar dynamics, which we have deduced from EPR spectroscopy. This point should be clarified by further experiments. Stacking order and disorder along the [001] direction, giving rise to different modifications, has been observed for $KCuF_3$ also, which similarly contains distorted CuF_6 octahedra in antiferrodistortive order (*13*).

In a very recent study on γ-$K_2PbCu(NO_2)_6$, based on single-crystal X-ray and neutron diffraction data, Yamada and co-workers propose a structural model, which is very similar to the antiferrodistortive pattern in Fig. 4 (*14*). In deviation from this pattern the K^+ and Pb^{2+} ions are slightly shifted away from the special positions ($\approx$4 pm) and the $Cu(NO_2)_6$ polyhedra are rotated around the c-axis by less than 2°, however. Possibly the low-temperature modifications of the Cs– and K–complexes are isostructural.

The neutron diffraction powder diagrams of $Cs_2CuPb(NO_2)_6$ within the stability range of the β'-phase still show a splitting of the orthorhombic 440 into monoclinic $\bar{4}40$ reflections. The corresponding very small deviation of γ from 90° was not detected because of experimental reasons by Mullen

TABLE III

STRUCTURAL DATA OF THE FOUR $Cs_2PbCu(NO_2)_6$ MODIFICATIONS [LATTICE PARAMETERS AND Cu–N BOND LENGTHS (pm)]

	a	b	c	(Cu–N)	T (K)	Space group
α	1097			217 $(6x)$	420	$Fm3$ (6)
β	1103	1100	1075	207 $(2x)^a$	323	$Fmmm$(5)
β'	1104	1101	1074	223 $(4x)^b$	293	$Fmmm$(4)[c]
γ^d	2194	2190	2138	207 $(2x)^a$	160	$B2/b$
	$\gamma = 90, 23°$			212 $(2x)^b$		
	773	1553	2138	230 $(2x)^c$		
	$\gamma' = 90, 10°$					

[a] Along the c-direction.

[b] In (001) planes.

[c] Monoclinic phase with very small deviation from $Fmmm$ (compare discussion); in (4) the notations β and β' have to be interchanged.

[d] Dimensions of the large $[2a, 2b, 2c, \gamma]$ and the smallest unit cell $[a', b', c', \gamma']$, respectively (compare Fig. 4).

et al. (4), who described the β'-structure in *Fmmm* (Table III).

Finally it should be noted that the magnetic structures of the Cu^{2+}–nitrocomplexes are equivalent in symmetry to the observed cooperative Jahn–Teller ordering patterns. This topic is discussed in a review, which deals with structural and bonding properties of Jahn–Teller unstable systems, in particular those of Cu^{2+}- and Co^{2+}–nitrocomplexes (3).

Acknowledgments

We must thank the Institut für Angewandte Kernphysik, Kernforschungszentrum Karlsruhe, for providing the working facilities for one of us (S. Klein) and Dr. P. Köhl for discussions.

References

1. D. REINEN, C. FRIEBEL, AND K. P. REETZ, *J. Solid State Chem.* **4**, 103 (1972).
2. C. FRIEBEL, *Z. Anorg. Allg. Chem.* **417**, 197 (1975).
3. D. REINEN AND C. FRIEBEL, "Structure Bonding," Vol. 37, Springer-Verlag, Berlin/New York, in press.
4. D. MULLEN, G. HEGER, AND D. REINEN, *Solid State Commun.* **17**, 1249 (1975).
5. R. HELMBOLD, D. MULLEN, H. AHSBAHS, A. KLOPSCH, E. HELLNER, AND G. HEGER, *Z. Kristallogr.* **143**, 220 (1976).
6. S. KLEIN AND D. REINEN, *J. Solid State Chem.* **25**, 295 (1978).
7. E. DUBLER, J. P. MATTHIEU, AND H. R. OSWALD, "Report, 4th International Conference on Thermal Analysis" (1974).
8. M. MORI, Y. NODA, AND Y. YAMADA, *Solid State Commun.* **27**, 735 (1978).
9. D. REINEN, *Solid State Commun.* **21**, 137 (1977).
10. S. KLEIN AND H. WEITZEL, *J. Appl. Crystallogr.* **8**, 54 (1975).
11. S. TAKAGI AND M. D. JOESTEN, *Acta Crystallogr. Sect. B* **31**, 596 (1975).
12. B. V. HARROWFIELD AND J. R. PILBROW, *J. Phys. C: Solid State Phys.* **6**, 755 (1973).
13. A. OKAZAKI, *J. Phys. Soc. Japan* **26**, 870 (1969).
14. V. NODA, M. MORI, AND Y. YAMADA, *J. Phys. Soc. Japan* **45**, 954 (1978).